RSC Advances

ROYAL SOCIETY OF CHEMISTRY

www.rsc.org/advances

RSC Advances

RSCPublishing

ARTICLE

Structural modifications induced by the switch from an endogenous bis-histidyl to an exogenous cyanomet hexa-coordination in a tetrameric haemoglobin

Cite this: DOI: 10.1039/xoxxoooooox

Received ooth April 2014,
Accepted ooth May 2014

DOI: 10.1039/xoxxoooooox

www.rsc.org/

Lelio Mazzarella [a], Antonello Merlino [a,b], Luigi Vitagliano [b], Cinzia Verde [c,d], Guido di Prisco [c], Jack Peisach [e], Alessandro Vergara [a,b*]

Ferric cold-adapted fish haemoglobins exhibit heterogeneous coordination at the α (aquo-met) and β (bis-histidyl) subunits. Herein we report two EPR-distinct bis-histidyl conformers (I and II) of the β subunits of ferric haemoglobin from *Trematomus bernacchii* which react differently with CN^-. An EPR titration reveals that upon cyanidation the most distorted conformer I reacts faster than II, producing both a cyanided and penta-coordinate ferric forms in the β subunits. The X-ray crystal structure of the partially cyanided conformer I reveals both an order-disorder transition and details of a communication between α and β subunits.

Introduction

In addition to the commonly observed aquo-met or hydroxyl-met species, oxidation of haemoglobins (Hbs) can lead to the formation of penta-coordinate and endogenous hexa-coordinate species, including bis-His adducts (hemichromes). It has been shown that hemichromes can be observed under non-denaturing as well as under physiological conditions both in mammals and fish [1, 2] Hbs. The physiological role of hemichromes is still disputed. It has been suggested that hemichromes can be involved in nitric oxide detoxification by acting as NO scavengers [3], in reduction of met-Hb *in vivo* [4], in Heinz body formation [5], in ligand binding [6], in modifying erythrocyte membrane rigidity [7] or in protection of Hb from peroxidation attack [8].

Several crystal structures of bis-histidyl adducts are available in the Hb superfamily, for either monomeric, dimeric and tetrameric Hb [1]. In the latter case, a partial hemichrome state has been observed in both mammalian and Antarctic fish Hbs. For crystalline horse Hb at acidic pH, the aquo-met form converts to one with α (bis-histidyl) and β (aquo-met) coordination [9]. A similar α (bis-histidyl) and β (aquo-met) coordination was recently observed also for a shark Hb [10]. On the other hand, crystallographic evidence revealed that ferric tetrameric Hbs isolated from Antarctic fish species (AFHbs) display an α (aquo-met) and β (bis-histidyl) coordination within a quaternary structure [11], herein denoted as H, which is intermediate between the classical R and T forms. Bis-histidyl coordination was recently also observed in a T-quaternary state, under strongly T-state stabilizing conditions [12]. The propensity to form a bis-His adduct at the β subunit of Hb from the Antarctic fish *Trematomus bernacchii* (HbTb) was recently assessed [13]. It was shown that there is an intrinsic propensity to form bis-His structure in the β subunit of HbTb, much more pronounced than in the β-subunit of human Hb [13, 14].

EPR analysis on several AFHbs and sub-Antarctic Hbs suggested the presence in frozen solution of two distinct hemichrome species (I and II) [11], presumably characterized by a different stereochemistry of the bis-His coordination at the heme [2, 11].

This work is intended to explore the reactivity of the bis-His adduct in tetrameric AFHbs, with special attention to α/β heterogeneity and heme-heme communication occurring during cyanidation. Up to now, endogenous-exogenous coordination substitution upon cyanidation has been investigated from a structural point of view in monomeric Hbs from *Synechosystis* [15] and *Drosophyla melanogaster* [16], and in dimeric *Caudina arenicola* Hb [17]. Since AFHb accommodates bis-histibyl coordination under physiological conditions, we chose HbTb as model system to investigate bis-histidyl reactivity in

tetrameric Hbs. Therefore, here we show the conformational changes occurring upon cyanidation of tetrameric HbTb, initially in a partial bis-His state. The crystallographic characterization is accompanied by EPR titration of HbTb with CN^-. Finally, we explore conformational changes occurring in a tetrameric Hb upon the conversion from endogenous to exogenous hexa coordination, showing a heme-heme communication mechanism related to the hemichrome reactivity.

Materials and Methods

EPR spectroscopy. HbTb, purified as previously reported [11], was fully oxidized with $K_3Fe(CN)_6$ and then titrated with increasing amounts of CN^-. Ferricyanide excess was removed from ferric HbTb by repeated G-25 Sephadex chromatographic runs, similar to a previous study on the ferric forms of HbTb [11]. Continuous wave EPR spectra were obtained at 12 K using a Varian E112 spectrometer equipped with a Systron-Donner frequency counter and a PC-based data acquisition program. The samples of ferric HbTb were at 0.5 mM tetramer concentration, in 50 mM Hepes pH 7.6. Spectra were recorded at a microwave frequency of 9.29 GHz, a microwave power of 10 mW, a modulation frequency of 100 kHz, and a modulation amplitude of 5 G.

X-ray crystallography. X-ray diffraction analysis was also conducted on crystals obtained from a preparation of ferric HbTb with CN^- in an CN^-:iron molar ratio of 1:2 (see below for rationale). Crystallization of partially cyanided HbTb (CN-HbTb) was carried out at pH 7.6 and room temperature by liquid-diffusion technique, using a capillary. The free interface diffusion technique was used by pouring the protein (final concentration 5 mg/ml) in 60 mM Tris-HCl (pH 7.6) on a solution containing 14% (w/v) MPEG 5000 into a capillary sealed in air at 20 °C. Diffraction data were collected at high resolution (1.54 Å) at the XRD1 beam-line of Elettra synchrotron. A data set was collected at 100 K using 22% glycerol as cryo-protectant and processed with the program suite HKL [18]. A summary of the data-processing statistics is given in Table S1. The coordinates of ferric HbTb at pH 7.6 [Protein Data Bank (PDB) code 2PEG] were used as a starting model to refine the structure of CN-HbTb. The refinement was performed using SHELXL [19]. The refinement runs were followed by manual intervention using the molecular graphic program O [20] to correct minor errors in the position of the side chains. At convergence, the R-factor value was 0.165 (R-free 0.197). A summary of the refinement statistics is reported in Table S1. The atomic coordinates have been deposited in the PDB, entry code 4ODC.

Results and discussion

EPR titration of a solution of HbTb with CN^- was performed at pH 7.6 (**Figure 1**). The spectrum of the starting sample of HbTb, preliminarily oxidized with $K_3Fe(CN)_6$, reveals the presence of several species. In particular, signals corresponding to aquomet (g values 5.88 and 2.01), hydroxymet (g values 2.6, 2.2) and two distinct hemichromes (I and II with g values 3.2, 2.2/2.3 and 2.9, 2.2/2.3, respectively) were detectable (**Figure 1**, spectrum A). Previous investigations have shown that the occurrence of two hemichromes (reported as I and II in Figure 1) is a common feature of AFHbs [11]. It was also suggested that the stereochemistry of hemichrome I is more distorted than that exhibited by hemichrome II [11].

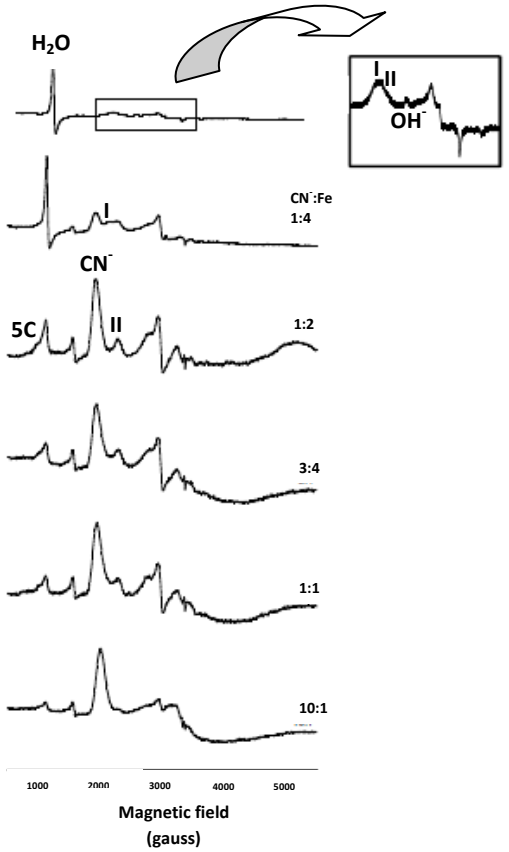

Fig. 1. EPR titration of ferric HbTb with CN^-. In the inset, the spectrum of ferric HbTb (top) in the low-spin region is expanded, showing the EPR signals of hemichrome I and II present in ferric HbTb frozen solution [2]. The molar ratio CN^-:iron is also reported for the 5 steps of CN^- titration. 5C stands for high-spin penta-coordinate heme

The progressive addition of CN^- produces significant changes in the EPR spectra. The addition of small amounts of CN^- (CN^-:iron molar ratio of 1:4) leads to a significant decrease of the aquomet, hydroxymet and hemichrome I species. In addition, a new low-spin signal (g=2.6, 2.2 and 1.8) is now resolved, and assigned to the cyano-met form. These trends are amplified upon a further increase of CN^- (ratio 1:2). Interestingly, at this molar ratio, hemichrome I is no longer present in the EPR spectrum, whereas no cyanidation of hemichrome II (g = 2.9, 2.3/2.2) occurs. Indeed, the signal corresponding to hemichrome II is not affected even when the iron:CN^- molar ratio is 1:1. Noteworthly, the 1:2 CN^-:iron

molar ratio corresponds to the condition used for the partially cyanided crystal structure herein reported. This unusual molar choice of our crystallographic work is justified by the intention to trap an intermediate cyanidation state in which hemichrome I is no longer present in the frozen solution used for EPR analysis. The EPR titration results clearly indicate that the two species have very different reactivity and are not in equilibrium. Indeed, this signal of hemichrome II, likely to represent a partially unfolded state, decreases only under high CN^- concentrations. A possible reason for such different reactivity between hemichrome I and II may be related to the unfolded globin state of the less abundant and less distorted hemichrome II [21].

The addition of CN^- also led to an increase in rhombicity of the high-spin signal. This is particularly evident in the spectrum at the ratio 1:2 as a shoulder of the aquomet signal. This shoulder is also detected in the spectra at ratio 3:4 and 1:1 but is no longer present at high CN^- concentration (ratio 1:10). In line with previous studies, this rhombicity may be confidently assigned to the formation of a penta-coordinate high-spin Fe(III) species [8]. The occurrence of a penta-coordinate ferric species is somewhat surprising. This clearly indicates that cyanidation of HbTb is not a simple replacement of the pre-existing ligands to the iron with CN^-. Instead, it is an intricate process in which at least four species (aquo-met, hemichrome I, penta-coordinate, CN-met) are implicated.

In order to shed light on the structural events involved in HbTb cyanidation, crystallization trails were set-up with the aim of obtaining crystals of intermediate species along this pathway. Crystals suitable for crystallographic analyses were grown from the mixture with an CN^-:iron molar ratio of 1:2. Luckily, despite the heterogeneity of this solution, highly ordered crystals diffracting at 1.54 Å were obtained. The electron density of the final model, hereafter denoted CN-HbTb, is generally well defined.

The inspection of the Fourier map at the heme pockets suggests that co-crystallizaton of more than one species has occurred. At the α-heme the electron density indicates that an exogenous ligand occupies the sixth coordination position of the iron (**Figure 2A**); the shape of the density is compatible with mixed aquo-/CN^- binding. All residues in the pocket are well defined and adopt the conformations normally detected in the R-state of tetrameric Hbs [22]. Analysis of the β-heme region (**Figure 2B**) shows that the pocket is significantly compressed when compared to the canonical R-state of carbomonoxy Hbs. Indeed, the distance between the Cα atoms of distal and proximal His in CN-HbTb, used as an indicator of the heme region in tetrameric Hbs, is 13.0 Å. This value is significantly lower than that observed (14.5 Å) in the canonical R and T state of HbTb [22-25], though higher than that observed with the formation of bis-His states in HbTb (12.5 Å) [11]. Analysis of the electron density of the β heme pocket shows the presence of a peak close to the heme iron, likely associated with the binding of an exogenous ligand. The distance between Nε of distal His (His63β) and the N atom of the cyanide ion is as low as 2.08 Å, compatible only with the presence of two alternative conformations, assignable to penta coordinate and cyano-met (**Figure 2B**), according to our EPR analysis. In addition, the density corresponding to the side chain of distal His (His63β) is somewhat elongated, suggesting that the residue adopts multiple rotameric states. Therefore, the density can be interpreted by assuming the presence in the crystal of two equally populated distinct states for this side chain: one His side chain points toward the heme (internal state), and a second side chain which swings out of the heme pocket (external state). Interestingly, due to the compression of the heme pocket the internal state of His63β is not compatible with the presence of an exogenous ligand to the iron. Taking also into account the EPR data, these findings have been interpreted by assuming in the crystal state the coexistences of two distinct states: (i) a hexacoordinate state with a CN^- ion bound to the iron and the distal His side chain protruding outside the pocket (external state), and (ii) a pentacoordinate state with the His63β side chain occupying the internal position. The analysis of the electron density and the limited entity of the pocket closure show that no bis-His adduct is present in the structure.

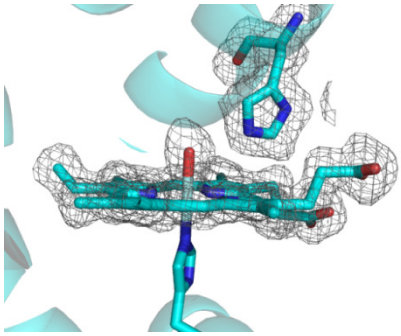

A

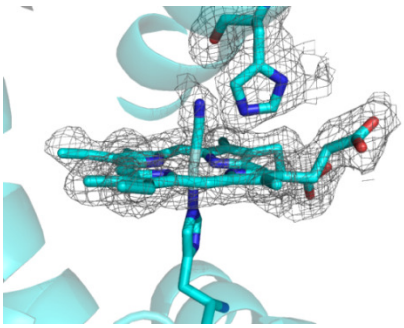

B

Fig. 2. Electron density maps near α (A) and β (B) hemes of CN-HbTb. For sake of clarity, at the α heme only aquo-met is reported, whereas at the β heme only the "internal state" conformation of distal His63β is shown (see below for definition). In Figure B the distance between Nε of His63β and the N atom of cyanide is too small (2.08 Å) to be physically incompatible, indicating the presence of two alternative conformations (penta-coordinate and cyano-met).

Altogether, these results indicate that a single quaternary structure of the protein is associated with different coordination states of the iron. Since (i) previous analyses on AFHbs have shown that the presence of a penta-coordinated state at the β iron is preferentially associated with a diatomic ligand bound to

the α heme [26, 27], and that (ii) our EPR data show no preferential cyanidation of aquomet and hemichrome I, we can conclude that the two species present in the crystal are $\alpha_{(CN-)}/\beta_{(penta)}$ and $\alpha_{(aquo)}/\beta_{(CN-)}$.

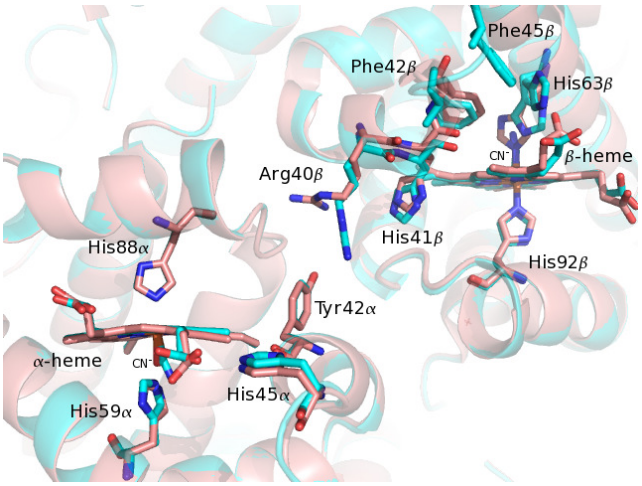

Fig. 3. Superimposition of hemi-HbTb (pink) and CN-HbTb (cyan), showing the α heme-β heme communication.

The quaternary structure of hemi-HbTb (pdb code 2PEG) does not change upon cyanidation (CN-HbTb), being still intermediate between the canonical R and T states [11]. The Cα root mean square deviations of the two models is as low as 0.37 Å. Details of the structural modifications occurring upon cyanidation of HbTb are shown in Figure 3. Interestingly, differences in tertiary structure between hemi-HbTb and CN-HbTb provide a possible mechanism of α and β cyanidation. The most relevant structural modification upon cyanidation is observed at the CDβ region, which becomes ordered in CN-HbTb. Indeed, upon β cyanidation, the swinging out of distal His63β pushes Phe45β far, modifying *via* residues 42β-41β the Arg40β side chain (**Figure 3**, S1 and S2). This residue is at the αβ interface and is in contact with the EFα region and with Tyr42α. These residues could modify, *via* His45α, the conformation of the α-heme propionate (**Figure S2**). Similarly, upon α cyanidation, the movement of distal His induces a shift of His45α, that *via* the Arg40β side chain could be transmitted to the CDβ region and thus to the β heme, with the reverse mechanism above described.

Conclusions

Altogether we state that diatomic ligands such as CN^- in β are not easily fully ligated within the H quaternary structure (associated with a tight heme pocket), and that the biatomic insertion in β hemes requires a movement of distal His that swings out of the heme pocket. A possible reason is the scissor-like motion required at the β heme upon T-H or R-H transition [11]. The evidence in AFHbs of an intermediate H quaternary state with a stable distal His rotamer that swings out is transferrable to a more general breathing mechanism of helices E and F of tetrameric Hbs coupled with the His motion, systematically observed as a transient form in the study of molecular dynamics of CO binding [28], and even observed in crystal structures of tetrameric Hbs [29].

Acknowledgements

This work was financially supported by PNRA (Italian National Programme for Antarctic Research). We thank the Elettra Synchrotron (Trieste, Italy) for beam-time and the staff of the beam-line XRD1 for assistance during data collection. AV acknowledges the University of Naples and the Albert Einstein College of Medicine for travel grants. Work carried out at AECOM was supported by National Institutes of Health grants GM040168 and HL071064-03004, awarded to JP.

Notes and references

[a] *Dept. of Chemical Sciences, University of Naples "Federico II", Naples, Italy. avergara@unina.it*
[b] *Institute of Biostructures and Bioimaging, CNR, Naples, Italy, luigi.vitagliano@unina.it*
[c] *Institute of Biosciences and BioResources, CNR, Naples, Italy, c.verde@ibp.cnr.it*
[d] *Roma 3 University, Dept. of Biology , Rome, Italy*
[e] *Dept. of Biophysics and Physiology, Albert Einstein College of Medicine, New York, NY, US.*

† Electronic Supplementary Information (ESI) available: [details of any supplementary information available should be included here]. See DOI: 10.1039/b000000x/

1 S. Kakar, F.G. Hoffman, J.F. Storz, M. Fabian, M.S Hargrove,. *Biophys. Chem.,* 2010, **152**, 1.
2 A. Merlino, B. Howes, C. Verde, G. di Prisco, G. Smulevich, L. Mazzarella, A. Vergara, *IUBMB life*, 2011, **63**, 295.
3 J. Wittenberg, B. Wittenberg, Q. Gibson, M. Trinick, C. Appleby, *J. Biol. Chem.,* 1986, **261**, 13624.
4 T.R. Weiland, S. Kundu, J.T. III Trent, J.A. Hoy, M.S. Hargrove, *J. Am. Chem. Soc.*, 2004, **126**, 11930.
5 J.M. Rifkind, O. Abugo, A. Levy, J.M. Heim, *Meth. Enzymol.*, 1994, **231**, 449.
6 A. Pesce, D. De Sanctis, M. Nardini, S. Dewilde, L. Moens, T. Hankeln, T. Burmester, P. Ascenzi, M. Bolognesi, *IUBMB Life*, 2004, **56**, 657.
7 F. Tokumasu, G.A. Nardone, G.R. Ostera, R.M. Fairhurst, S.D. Beaudry, E. Hayakawa, J.A. Dvorak, *PLoS One,* 2009, **4**, 1.
8 A. Vergara, M. Franzese, A. Merlino, G. Bonomi, C. Verde, D. Giordano, G. di Prisco, H.C. Lee, J. Peisach, L. Mazzarella, *Biophys. J.*, 2009, **97**, 866.
9 V.L. Robinson, B.B. Smith, A. Arnone, *Biochemistry*, 2003, **42**, 10113.
10 P Ramesh, S.S. Sundaresan, P.S. Moorthy, M. Balasubramanian, M.N. Ponnnuswamy, *J. Synchrotron Rad.*, 2013, **20**, 843.
11 A. Vergara, M. Franzese, A. Merlino, L. Vitagliano, C. Verde, G. di Prisco, H.C. Lee, J. Peisach, L. Mazzarella, *Biophys. J.*, 2007, **93** 2822.
12 L. Ronda, A. Merlino, S. Bettati, C. Verde, A. Balsamo, L. Mazzarella, A. Mozzarelli, A. Vergara, *BBA Prot. & Proteomics*, 2013, **1834**, 1885.
13 A. Balsamo, F. Sannino, A. Merlino, E. Parrilli, M.L. Tutino, L. Mazzarella, A. Vergara, *Biochimie,* 2012, **94**, 953.
14 E.A. Rachmilewitz, J. Peisach, W.E. Blumberg., *J. Biol. Chem.*, 1971, **246**, 3356.
15 J.T. 3rd Trent, S. Kundu, J.A. Hoy, M.S. Hargrove, *J Mol Biol.*, 2004, **341**, 1097.
16 D. de Sanctis, P. Ascenzi, A. Bocedi, S. Dewilde, T. Burmester, T. Hankeln, L. Moens and M. Bolognesi, *Biochemistry,* 2006, **45**, 10054.
17 D.T. Mitchell, G.B. Kitto, M.L. Hackert., *J. Mol. Biol.,* 1995, **251**, 421.
18 Z. Otwinowski, W. Minor, *Meth. Enz.,* 1997, **276**(part A), 307.
19 G.M. Sheldrick, *Acta Cryst.*, (2008) **D64**, 112.

20 T.A. Jones, M. Kjeldgaard, Essential O, software manual, Uppsala (pp. 178). 1988.
21 A. Vergara, L. Vitagliano, C. Verde, G. di Prisco, L. Mazzarella, *Meth. Enz.*, 2008, **436**, 425, 56.
22 L. Camardella, C. Caruso, R. D'Avino, G. di Prisco, B. Rutigliano, M. Tamburrini, G. Fermi, M.F. Perutz, *J. Mol. Biol.,* 1992, **224**, 449.
23 L. Mazzarella, A. Vergara, L. Vitagliano, A. Merlino, G. Bonomi, S. Scala, C. Verde, G. di Prisco, *Proteins Str. Funct. Bioinf.,* 2006, **65**, 490.
24 A. Vergara, L. Vitagliano, K. Marino, A. Merlino, F. Sica, C. Verde, G. di Prisco, L. Mazzarella, *J. Biol. Chem.,* 2010, **285**, 32568.
25 C. Verde, A. Vergara, L. Mazzarella, G. di Prisco, *Curr. Prot. Pept. Sci.*, 2008, **9**, 578.
26 L. Vitagliano, A. Vergara, G. Bonomi, A. Merlino, C. Verde, G. di Prisco, B.D. Howes, G. Smulevich, L. Mazzarella, *J. Am. Chem. Soc.*, 2008, **130**, 10527.
27 A. Merlino, L. Vitagliano, B.D. Howes, C. Verde, G. di Prisco, G. Smulevich, F. Sica, A. Vergara, *Biopolymers,* 2009, **91**, 1117.
28 L. Capece, L. Boechi, L.L. Perissinotti, P. Arroyo-Mañez, D.E. Bikiel, G. Smulevich, M.A. Marti, D.A. Estrin, *Biochim. Biophys. Acta,* 2013, **1834**, 1722; 57.
29 J.D. Jenkins, F.N. Musayev, R. Danso-Danquah, D.J. Abraham, M.K. Safo, *Acta Cryst*., 2009, **D65**, 41.

Lelio Mazzarella, et al. "**Structural modifications induced by the switch from an endogenous bis-histidyl to an exogenous cyanomet hexa-coordination in a tetrameric haemoglobin"**

Text:

Two EPR- and structurally-distinct bis-histidyl conformers of the ferric haemoglobin from *Trematomus bernacchii* react differently with CN^-